PAPER

Check for updates

An ionic liquid–molecularly imprinted composite based on graphene oxide for the specific recognition and extraction of cancer antigen 153

Shuang Han, [ID] *[ab] Aixin Yao[a] and Yuan Wang[c]

Molecularly imprinted polymers with graphene oxide (GO) as a carrier (GMIPs) were synthesized to selectively recognize and capture cancer antigen 153 (CA153). The results show that the MIP has good selectivity and adsorption for CA153, and has strong anti-interference ability. Molecularly imprinted solid phase extraction (MISPE) combined with ultra performance liquid chromatography (UPLC) for the specific adsorption of CA153 was also established, and showed great potential for the analysis of CA153 in clinics in the future.

1. Introduction

Tumor markers (TMs) are compounds connected with tumor cells, and their quantification is significant for the diagnosis and clinical therapy of cancer patients. Cancer antigen 153 (CA153) is a macromolecular glycoprotein tumor marker associated with breast cancer and levels of it can be used as the best index to monitor the recurrence of breast cancer after operation.[1,2]

At present, the detection of glycoprotein tumor biomarkers is mostly by immunoassays, as they have the advantages of sensitivity and selectivity. However, the drawbacks of immunoassays, for example, the instability of the reagents and the high cost caused by the dependence on antibodies, have influenced their further applications in clinical analysis. In recent years, in order to effectively solve the problem of antibody dependence in traditional immunoassay methods, some antibody free bioanalysis methods, including spectrophotometry sensors and HPLC-based antibody-free immunoassays, have been developed.[3] However, their accuracy and sensitivity are always impacted by the low concentration of tumor biomarkers and the interference of high-abundance proteins which limits their accuracy and sensitivity. Moreover, most of these procedures are quite laborious. Therefore a novel pretreatment that has high selectivity, stability, simple operation and good anti-interference ability for glycoprotein tumor biomarkers is important to solve these drawbacks for antibody-free analysis.[4]

Molecular imprinting is an attractive technique to prepare highly selective polymers which have synthesized binding sites and can rebind specifically with a template molecule. The obtained molecularly imprinted polymers (MIPs) are stable, robust, and low cost.[5–7] Thus, using MIPs as selective adsorbent materials could clean-up and enrich targets from complicated samples, such as urine, before determination.

Although MIPs have excellent performance in many applications, they are often affected by the existence of heterogeneous molecular cavities and slow response time. Molecularly imprinted polymers have rarely used biomacromolecules as templates because some challenges have been found in the process of biomacromolecular imprinting. Firstly, the harsh conditions of polymerization may induce an irreversible structural change in CA153, resulting in weak selectivity. Secondly, the thorough elimination of the target template from the polymer to produce imprinted cavities is difficult with a large molecular size.[8,9] Thus, the development of molecularly imprinted polymers suitable for biomolecules would have an important impact on the development of molecularly imprinted technology, and is the focus of this study. Recently, the use of ionic liquids (ILs) in the field of enzyme and protein stabilization has attracted considerable attention.[10,11] It has been shown that ionic liquids as special functional materials have highly ordered anionic and cationic structures, which can help to increase the amount of bound water in aqueous solution and stabilize the conformation of proteins in aqueous phase. Therefore, it is expected that the problem of the conformation variability of protein macromolecules in the preparation of imprinted polymers can be solved by using ionic liquids as stabilizers. For example, Wang *et al.*[12] used ILs to maintain the structure and activity of proteins to prepare a molecularly imprinted film on an electrode surface for human epididymis protein 4 (HE4) sensing.

[a]College of Chemistry and Chemical Engineering, Qiqihar University, Qiqihar, 161006, China

[b]Heilongjiang Provincial Key Laboratory of Catalytic Synthesis for Fine Chemicals, Qiqihar University, Qiqihar, 161006, China

[c]Heilongjiang Province Qiqihar Ecological Environment Monitoring Center, Qiqihar, 161005, China

Using graphene oxide (GO), which has a large area and unique electrical performance, as an excellent carrier material for the preparation of MIP-based materials may avoid these undesired effects.[13,14] Several research groups have already synthesized composites making use of the desirable combination of GO and MIPs to improve the selectivity and binding dynamics of MIPs.[15]

In the present work, we used GO as the support material, an IL as the stabilizer, CA153 as the template and DA as the functional monomer in the presence of cross-linkers for the preparation of MIPs based on GO (GMIPs). The synthesized hybrid, integrating the selectivity of MIPs and the special properties of GO and the IL, presented specific and fast adsorption for CA153. The route of the preparation process is presented in Fig. 1. The GO surface contains a large number of –OH, –COOH and other functional groups. Dopamine (DA) can adhere to almost all substrates such as GO, metal, SiO_2, wood, Fe_3O_4 and glass through a rapid self-aggregation reaction.[16,17] The hydroxyl and amide functional groups of DA would form non-covalent interactions with CA153. After binding to the template, a surface imprinted layer of DA was formed on GO. After removing CA153, GMIPs with imprinted cavities inside or on the surface of the polymer which were complementary in size, shape and functional groups to the template CA153 were obtained. The prepared polymers were used as solid phase extraction (SPE) materials and were applied to the selective extraction of CA153 from human urine. Some factors effecting polymerization and the extraction process were investigated and optimized. To the best of our knowledge, this is the first report of molecularly imprinted SPE materials coupled to UPLC for the enrichment and determination of CA153. The method proposed a simple and novel way for the pretreatment of CA153 from biological samples.

2. Experimental

2.1. Materials and reagents

Dopamine (DA) and dimethyl sulfoxide (DMSO) were purchased from the Shanghai Aladdin Bio-Chem. Technology Corporation (Shanghai, China). Cancer antigen 153 (CA153),

Fig. 1 Schematic illustration of the preparation of GMIPs.

immunoglobulin (IgG), glucose (Glu) and histidine (His) were obtained from Shanghai Linc-Bio Science Co. Ltd (Shanghai, China).

2.2. Preparation of GMIPs

GO was prepared by a modified Hummers method.[18] The preparation scheme of the GMIP hybrid is as follows. At the beginning, 1.0 g of GO was added into 25 mL of 200 mM phosphate buffer (pH 8.5). Then, 5 mmol 1-butyl-3-methylimidazolium chloride (IL) and 10 mg DA were dissolved in the mixture. Next, 50 μL of CA153 and 10 mg of ammonium persulfate (APs) were added to the above mixture and polymerized at room temperature for 1 hour. After the polymerization, the polymer was washed with ethanol to remove CA153. The corresponding non imprinted polymers (GNIPs) were prepared similarly to the GMIPs but without the addition of CA153. For comparison, MIPs and GMIPs (without the IL) were also prepared similarly to GMIPs except without the addition of graphene oxide and IL, respectively.

2.3. Apparatus

Scanning electron microscope (SEM) pictures were taken with a Japan HITACHI S-4300 scanning electron microscope. The X-ray diffraction (XRD) patterns were measured using a Bruker-D8 focal X-ray diffractometer. UPLC determination was performed on the Waters ACQUITY UPLC system containing an ACQUITY UPLC-BEH column (100 mm × 2.1 mm, 1.7 μm).

2.4. Adsorption experiment

5.0 mg of GMIPs, MIPs or GNIPs was added to 5 mL of 0.5 mg L^{-1} CA153 solution. When equilibrium was reached, the GMIPs or GNIPs were removed, and the binding amount of the template to the polymer was determined according to the concentration difference before and after adsorption, calculated by UPLC analysis. The adsorption capacity (Q) was determined by the following equation:

$$Q = (C_1 - C_2) \times V/W \tag{1}$$

where C_1 and C_2 are the CA153 concentration before and after binding, respectively, V is the volume of liquid and W is the amount of GMIPs, MIPs or GNIPs.

2.5. Selectivity binding experiments

5 mg of GMIPs or GNIPs were mixed with 5 mL of 0.5 mg L^{-1} CA153, His, Glu and IgG solutions. The experiment was the same as the previous adsorption experiment.

2.6. Preparation and chromatographic conditions of MISPE

An aliquot (1–8 mL) of human urine was spiked with 0.4 mol L^{-1} of CA153 phosphate buffer solution (the same volume as the urine sample). 0.1 g of the GMIP composite was packed in an empty column as the molecularly imprinted solid phase extraction (MISPE) material. The MISPE cartridge was continuously treated with 10 mL methanol and 10 mL water and then
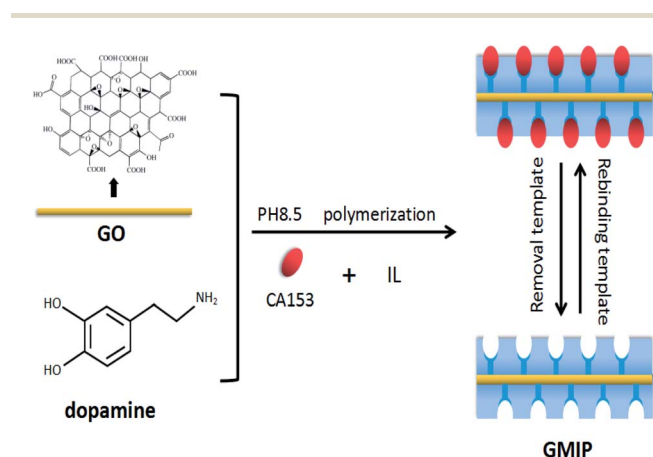
the spiked sample was passed through the cartridge at a flow rate of 0.5–3.0 mL min^{-1}. The extract was then eluted with acetonitrile/acetic acid (acetonitrile : acetic acid = 90 : 10, v/v). Finally, the extract was purged to a final volume of 0.5 mL under nitrogen for subsequent UPLC analysis at 294 nm with a flow rate of 0.5 mL min^{-1}. All of the substances were detected using the optimal UPLC mobile phase (methanol : HAc : H$_2$O = 85 : 1 : 14). The use of all urine samples in this study complied with the current ethical considerations and received the approval of the Ethics Committee of Qiqihar University. Informed consent was obtained from human participants of this study.

3.   Results and discussion

3.1.   Optimization of imprinting

In order to obtain the best binding capacity of GMIPs to the template CA153 molecules, the concentration of the IL during the process of molecularly imprinted polymerization was optimized by a binding experiment (Fig. 2). With the increase of the IL content the adsorption capacity of the GMIPs firstly increased and then decreased gradually after the content of the IL exceeded 5 mmol. This might be because at the optimum amount of the IL, the presence of the IL was favourable for the stability of the CA153 molecules during the process of polymerization. However, much more of the IL may decrease the polymeric degree, leading to a structure with poor rigidity.

3.2.   Characterization of the GMIPs

Under SEM observation (Fig. 3), the GMIP nanoparticles had a fine spherical shape with uniform size distribution. The spherical geometry and the monodispersion of the prepared microspheres increased the surface area. The surfaces of the GMIP and MIP were rougher than that of the GNIP, owing to the imprinted sites that were left after the removal of the template molecules. The GMIP showed less agglomeration than the MIP due to the presence of GO.

Fig. 4 shows the XRD patterns of GO and the GMIP. The diffraction peak at $2\theta = 11°$ is attributed to the (002) crystal of
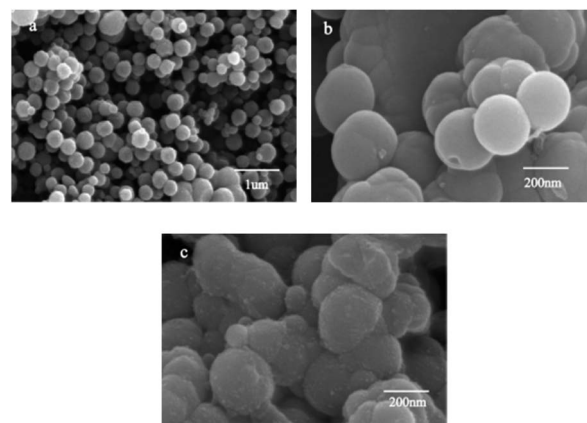

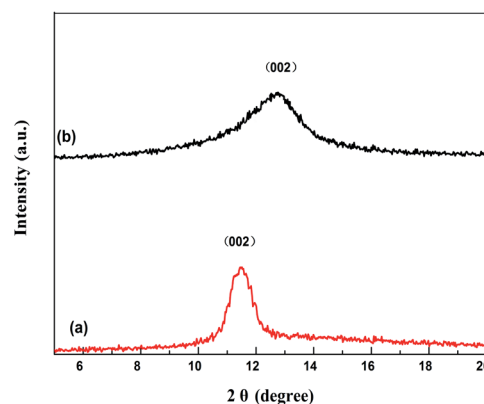Fig. 3   SEM images of the GMIP (a), GNIP (b) and MIP (c).

Fig. 4   XRD patterns of GO (a) and the GMIP (b).

GO.[19] The characteristic peak of GO is shown and the peak position is the same although its intensity decreases (curve b), which illustrates that the crystal structure of GO is intact.

GO and the GMIP were studied by Raman spectroscopy and the results are shown in Fig. 5. In curve a of Fig. 5, the D band (1338 cm^{-1}) and G band (1594 cm^{-1}) of GO can be observed, corresponding to disordered carbon and sp^2 hybridized carbon, respectively. These peak positions did not shift for the GMIP,
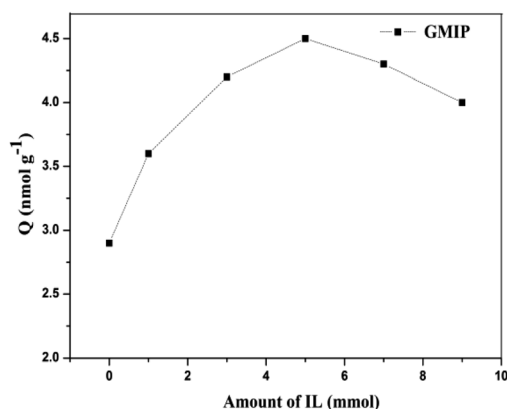

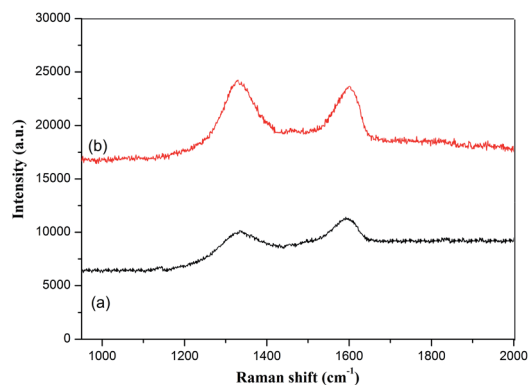Fig. 2   Effect of the amount of the IL on the adsorption capacity of GMIPs for CA153.

Fig. 5   Raman spectra of GO (a) and the GMIP (b).

Table 1 Surface properties of the GMIP, GNIP and MIP

Polymer	BET surface area ($m^2 g^{-1}$)	Pore volume ($cm^2 g^{-1}$)	Pore size (nm)
GMIP	875.263	0.796	15.310
GNIP	365.142	0.313	17.996
MIP	612.321	0.553	16.103

while the ratio of $I(D)$ to $I(G)$ increased. Generally, the increase of the ratio of $I(D)$ to $I(G)$ reflects an increase in disorder in materials.[20] Therefore the enhanced rate of the GMIP can be attributed to the increase of the disorder degree of the materials due to the coating of the imprinted polymer film. The above research verified the successful preparation of the GMIP.

The BET surface areas of the as-synthesized GMIP and GNIP were found to be 875.263 $m^2 g^{-1}$ and 365.142 $m^2 g^{-1}$ (Table 1). The GMIP has larger surface area than the GNIP due to the removal of CA153 after polymerization. At the same time, the larger surface area of the GMIP than the MIP may be ascribed to the presence of more imprinted cavities exposed on the GO substrate. The much larger surface area of the GMIP is advantageous for the binding and encapsulation of the target CA153 molecules.

Fig. 6 shows the TGA curves for GO and the GMIP. For the GMIP, the weight loss below 120 °C can be attributed to the loss of residual or absorbed solvents. After that, sudden weight loss occurred from 300 °C to 530 °C, which might be related to the degradation of the carbon skeleton of the molecularly imprinted membrane. In addition, the total weight loss of the GMIP was significantly higher than that of GO, indicating that the MIP was successfully synthesized.

The FT-IR spectra of the GMIP and the MIP are shown in Fig. 7. The presence of the characteristic peak at 1450 cm^{-1} (N–H bending vibration) for both the GMIP and the MIP verified the presence of DA in the GMIP and the MIP. Compared to the MIP, the characteristic peak at 3400 cm^{-1} (–OH stretching vibration) was stronger, and a peak at 1730 cm^{-1} (the characteristic peak of C=O) appears for the GMIP, demonstrating the GO grafting to the imprinted polymers.
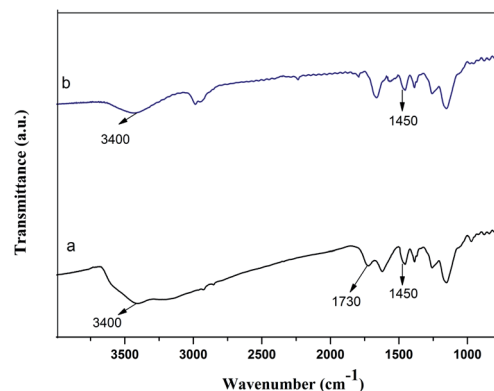

Fig. 7 FT-IR spectra of the GMIP (a) and the MIP (b).

3.3. Adsorption kinetics

The adsorption capacity of the GMIP for CA153 increased quickly with increasing adsorption time in the initial 15 min, and after that the curve was smooth (Fig. 8). Thus, the GMIP polymers had a fast adsorption speed for CA153 and the response of the GMIP was faster than that of the MIP. The adsorption capacity of the GMIP (4.5 nmol g^{-1}) was much higher than those of the MIP and the GNIP. The above results verified that the integration of GO in the GMIP had improved the properties of the binding kinetics to enhance the mass transfer speed and binding capacity. The adsorption of the GMIP was higher than the GMIP without the IL. This result may be ascribed to the IL being in favour of the stability of the CA153 molecules during the process of polymerization to form the imprinted cavities. Owing to the imprinted template cavities on the surface, CA153 could selectively bind to the GMIP compared to the GNIP.

3.4. Selectivity of the GMIP

The selectivity of the GMIP plays a very important role for specific recognition in biological samples, which are composed of several potential interferences, including compounds (Glu), proteins (Glo, IgG) and other amino acids (His). As shown in Fig. 9, the binding capacity of the GMIP for CA153 was significantly higher than that for other substances.
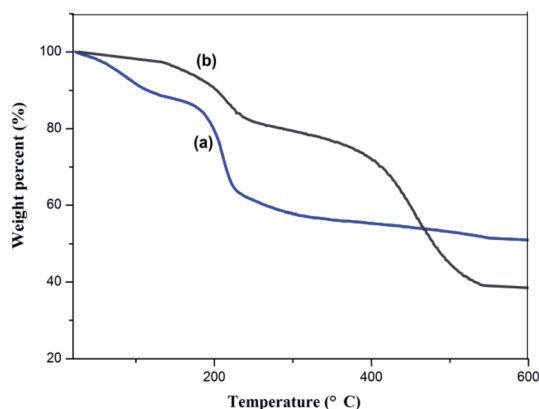

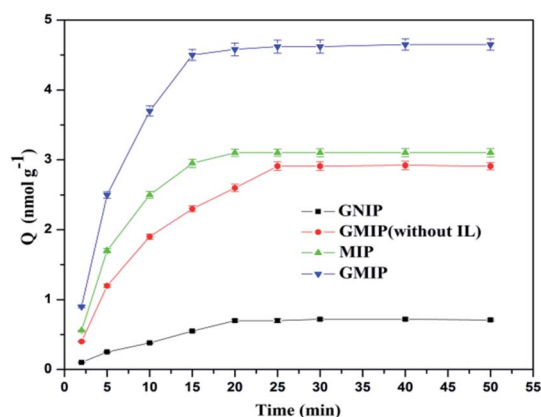**Fig. 6** TGA curves of GO (a) and the GMIP (b).

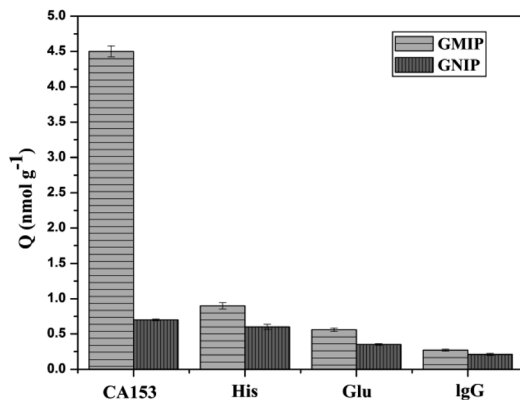**Fig. 8** Response time of the different polymers for CA153.

Fig. 9 Absorption capacities of the GMIP and the GNIP for different targets.

However, it can be seen that the binding ability of the GNIP with all objects is very poor, indicating that the GNIP has no specificity for CA153. Here, the imprinting factor was calculated using the ratio of adsorption of the GMIP for CA153 to that of the GNIP. The results show that the value is 6.42, suggesting the selectivity of the GMIP for CA153. The above phenomenon could be attributed to the existence of CA153 imprinted cavities in the GMIP, which can recognize CA153 from other molecules by their size, shape, functional groups and specific binding interactions. The GMIPs with high selectivity can be applied for the direct recognition of CA153 from complex matrices without separation.

3.5. MISPE-UPLC determination of CA153

3.5.1 Optimization of MISPE performance. The influence of the sample volume was considered in the range from 2 to 16 mL. As shown in Fig. 10, when the sample volumes were increased up to 12 mL an acceptable recovery rate was evident. Under these conditions, 12 mL is the tolerated volume for breakthrough. Therefore, 12 mL is the best sample volume.

In generally, a higher injection flow rate will shorten the interaction time between the analytes and the adsorbent and reduce the recovery of the analytes, while a low flow rate can lead to inefficiency. It was found that the recovery of CA153
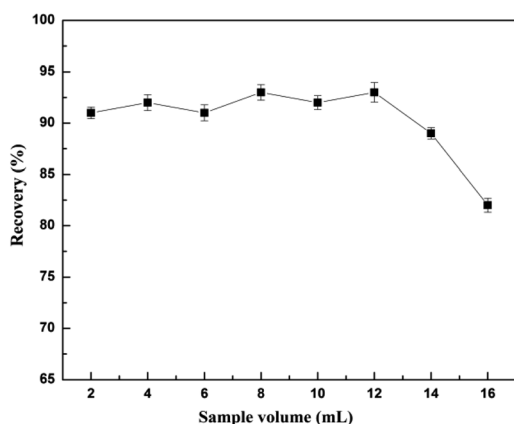

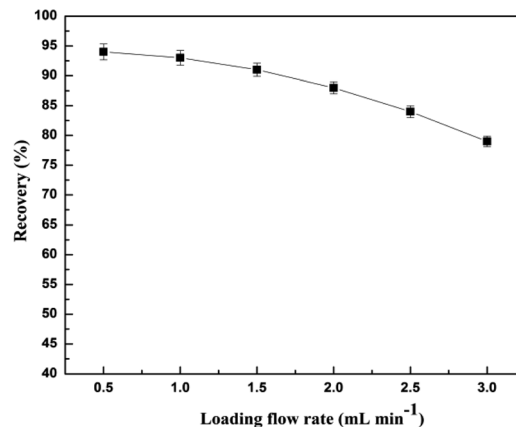Fig. 10 Effects of sample volume on recovery.

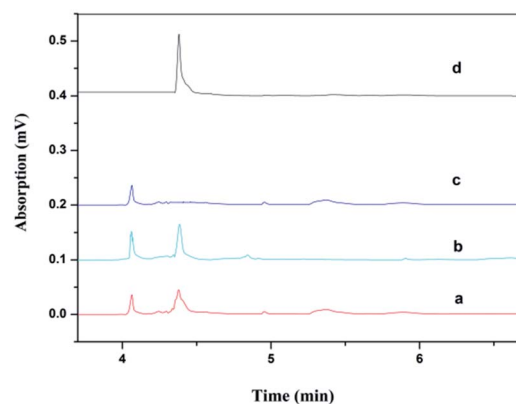Fig. 11 Effects of the loading flow rate on the recovery.

Fig. 12 Chromatograms of urine samples containing 0.2 mol L^{-1} of CA153 (a), urine samples (c), human urine sample spiked with CA153 after the GNIP SPE procedure (b) and the GMIP SPE procedure (d).

decreased with the increase of flow rate from 0.5 to 1.5 mL min^{-1}, and decreased significantly with the flow rate of the sample increasing from 1.5 to 3.0 mL min^{-1} (Fig. 11). Therefore, a flow rate of 1.5 mL min^{-1} was chosen.

3.5.2 Application of MISPE-UPLC. Next, the extraction of GA153 from a human urine sample was realized using the MISPE cartridge. Fig. 12 presents the chromatograms of the human urine sample spiked with CA153 and the elution through the MISPE procedure. According to the figure, CA153 was selectively retained by the GMIP, demonstrating that the GMIP led to CA153 being pre-concentrated, and at the same time interfering molecules were excluded from the polymer. The extraction recovery in urine samples was 90% for the GMIP. However, the pre-treatment obtained by the SPE procedure using the GMIP adsorbent was much better than that using the GNIP adsorbent. According to this method, specific enrichment and purification were achieved.

4. Conclusion

In this paper, a GMIP composite was prepared by combining the advantages of the high selectivity of molecularly imprinted

polymers with GO as a substrate and an IL as a stabilizer. In addition, because of presence of GO in the GMIP, the GMIP has the characteristics of fast adsorption kinetics and a large adsorption capacity. The GMIP was successfully used as an enrichment agent followed by UPLC for the selective enrichment and determination of CA153.

Conflicts of interest

There are no conflicts to declare.

Acknowledgements

References

1 W. Wang, X. Xu, B. Tian, et al., The diagnostic value of serum tumor markers CEA, CA19-9, CA125, CA15-3, and TPS in metastatic breast cancer, Clin. Chim. Acta, 2017, 470, 51–55.

2 S. Eun Nam, W. Lim, J. Jeong, et al., The prognostic significance of preoperative tumor marker (CEA, CA15-3) elevation in breast cancer patients: data from the Korean Breast Cancer Society Registry, Breast Cancer Res. Treat., 2019, 177(3), 669–678.

3 B. Babamiri, R. Hallaj and A. Salimi, Ultrasensitive electrochemiluminescence immunoassay for simultaneous determination of CA125 and CA15-3 tumor markers based on PAMAM-sulfanilic acid-Ru (bpy) 32+ and PAMAM-CdTe@CdS nanocomposite, Biosens. Bioelectron., 2018, 99, 353–360.

4 S. Han, Q. L. Su, H. Chu, et al., Two-dimensional molecularly imprinted photonic crystal sensor for highly efficient tetracycline detection, Anal. Methods, 2020, 12, 1374–1379.

5 F. Wang, B. Ling, Q. Li, et al., Dual roles of 3-aminopropyltriethoxysilane in preparing molecularly imprinted silica particles for specific recognition of target molecules, RSC Adv., 2020, 10, 20368–20373.

6 S. Han, L. Su, M. Zhai, et al., A molecularly imprinted composite based on graphene oxide for targeted drug delivery to tumor cells, J. Mater. Sci., 2019, 54(4), 3331–3341.

7 F. Wang, D. Wang, T. Wang, et al., A simple approach to prepare fluorescent molecularly imprinted nanoparticles, RSC Adv., 2021, 11, 7732–7737.

8 F. Barahona, B. Albero, J. L. Tadeo, et al., Molecularly imprinted polymer-hollow fiber microextraction of hydrophilic fluoroquinolone antibiotics in environmental waters and urine samples, J. Chromatogr. A, 2019, 1587, 42–49.

9 S. P. M. Ventura, F. A. e Silva, M. V. Quental, et al., Ionic-liquid-mediated extraction and separation processes for bioactive compounds: past, present, and future trends, Chem. Rev., 2017, 117(10), 6984–7052.

10 Z. He and P. Alexandridis, Ionic liquid and nanoparticle hybrid systems: emerging applications, Adv. Colloid Interface Sci., 2017, 244, 54–70.

11 S. Jafari, M. Dehghani, N. Nasirizadeh, et al., An azithromycin electrochemical sensor based on an aniline MIP film electropolymerized on a gold nano urchins/graphene oxide modified glassy carbon electrode, J. Electroanal. Chem., 2018, 829, 27–34.

12 C. Wang, X. Ye, Z. Wang, et al., Molecularly imprinted photo-electrochemical sensor for human epididymis protein 4 based on polymerized ionic liquid hydrogel and gold nanoparticle/ZnCdHgSe quantum dots composite film, Anal. Chem., 2017, 89(22), 12391–12398.

13 P. Dramou, A. Itatahine, M. Fizir, et al., Progress in the functional modification of graphene/graphene oxide: a review, RSC Adv., 2020, 10, 15328–15345.

14 S. Han, F. Teng, Y. Wang, et al., Drug-loaded dual targeting graphene oxide-based molecularly imprinted composite and recognition of carcino-embryonic antigen, RSC Adv., 2020, 10, 10980–10988.

15 S. Jafari, M. Dehghani, N. Nasirizadeh, et al., Label-free electrochemical detection of Cloxacillin antibiotic in milk samples based on molecularly imprinted polymer and graphene oxide-gold nanocomposite, Measurement, 2019, 145, 22–29.

16 H. Lee, S. M. Dellatore, W. M. Miller, et al., Mussel-inspired surface chemistry for multifunctional coatings, Science, 2007, 318(5849), 426–430.

17 Y. Qian, Y. Yuan, H. Wang, et al., Highly efficient uranium adsorption by salicylaldoxime/polydopamine graphene oxide nanocomposites, J. Mater. Chem. A, 2018, 6(48), 24676–24685.

18 S. N. Alam, N. Sharma and L. Kumar, Synthesis of graphene oxide (GO) by modified hummers method and its thermal reduction to obtain reduced graphene oxide (rGO), Graphene, 2017, 6(1), 1–18.

19 L. Dong, J. Yang, M. Chhowalla, et al., Synthesis and reduction of large sized graphene oxide sheets, Chem. Soc. Rev., 2017, 46(23), 7306–7316.

20 S. Hua, L. Zhao, L. Cao, et al., Fabrication and evaluation of hollow surface molecularly imprinted polymer for rapid and selective adsorption of dibenzothiophene, Chem. Eng. J., 2018, 345, 414–424.